Available online at www.sciencedirect.com
ScienceDirect
Journal of Magnetic Resonance 185 (2007) 103–109
JMR Journal of Magnetic Resonance
www.elsevier.com/locate/jmr

A study of tablet dissolution by magnetic resonance electric current density imaging

Urša Mikac [a,*], Alojz Demsar [b], Franci Demsar [a], Igor Serša [a]

[a] *Jožef Stefan Institute, Jamova 39, 1000 Ljubljana, Slovenia*
[b] *Faculty of Chemistry and Chemical Technology, University of Ljubljana, Ljubljana, Slovenia*

Received 24 July 2006; revised 16 November 2006
Available online 21 December 2006

Abstract

The electric current density imaging technique (CDI) was used to monitor the dissolution of ion releasing tablets (made of various carboxylic acids and of sodium chloride) by following conductivity changes in an agar–agar gel surrounding the tablet. Conductivity changes in the sample were used to calculate spatial and temporal changes of ionic concentrations in the sample. The experimental data for ion migration were compared to a mathematical model based on a solution of the diffusion equation with moving boundary conditions for the tablet geometry. Diffusion constants for different acids were determined by fitting the model to the experimental data. The experiments with dissolving tablets were used to demonstrate the potential of the CDI technique for measurement of ion concentration in the vicinity of ion releasing samples.

Keywords: Magnetic resonance imaging (MRI); Current density imaging (CDI); Dissolution process; Ion diffusion

1. Introduction

Electric current density imaging (CDI) is a magnetic resonance imaging (MRI) technique that images the induced electric current density and electric conductivity distribution within any sample containing water with mobile ions [1,2]. The intensity of the CD image is proportional to the electric current flowing through the sample. The sensitivity of the CDI technique depends on the sample impedance, the applied voltage, the total duration of current pulses, and the signal to noise ratio of the conventional MR image [3,4]. Sensitivity and resolution studies of the CDI method on a model sample showed that with a properly chosen electric current density and electric current pulse duration, the signal to noise ratio of the electric current density image is comparable to the signal to noise ratio of conventional images.

CDI can measure the electric current density in three different frequency ranges: at zero frequency using the direct current density imaging technique, DC-CDI [1,2], in the kiloHertz frequency range using the alternating current density imaging technique, AC-CDI [5], and at the Larmor frequency using the radiofrequency current density imaging technique, RF-CDI [6,7]. The methods have been used to image current distribution *in vitro* [8–11], to monitor chemical processes [12,13] and also to image current pathways and tissue conductivity *in vivo* [14–18].

Among its pharmaceutical properties, the disintegration and dissolution properties of a tablet, as well as the free diffusion of substances, are of considerable importance. In recent years increasing attention has been paid to development of tablets which can rapidly dissolve or disintegrate in the mouth. The impact of fast disintegrants [19,20], the procedure used for tablet preparation [21,22] and ageing [23–25] on the dissolution of a tablet are of a great interest. The aspirin tablet matrix was proposed as a model formulation for comparison of disintegrant efficiency and testing the performance consistency for quality control purposes [20].

* Corresponding author. Fax: +386 1 477 3191.
E-mail address: urska.mikac@ijs.si (U. Mikac).

1090-7807/$ - see front matter © 2006 Elsevier Inc. All rights reserved.
doi:10.1016/j.jmr.2006.12.002

In this paper, the feasibility of the CDI method for monitoring dissolution processes in tablets was studied. Electric conductivity images, acquired by the DC-CDI method, were used for tracing the dissolution of tablets and ion migration processes. The diffusion coefficients of various acids (tartaric, citric, oxalic, and maleic) and sodium chloride (NaCl) were determined from the CD image signal intensity acquired at different times after the beginning of the dissolution process.

2. Theory

The surface of a tablet that is in contact with an aqueous medium disintegrates into granules that in turn disaggregate into fine particles. Let us assume that the threshold concentration at which ions are formed and can be imaged by CDI is C_N. In our experiments, dissolution at the top and bottom of the tablet was obstructed because the samples were capped at the ends with electrodes. Additionally, the sample tablets had cylindrical symmetry so that ion migration and diffusion was only radially dependent (Fig. 1).

The mathematical model is divided into two parts. The first part corresponds to the time from the beginning of the experiment until the tablet is completely dissolved ($0 < t < t_0$) and considers tablet dissolution as well as ion diffusion, while the second part corresponds to time after the tablet is completely dissolved ($t > t_0$) and considers only ion diffusion.

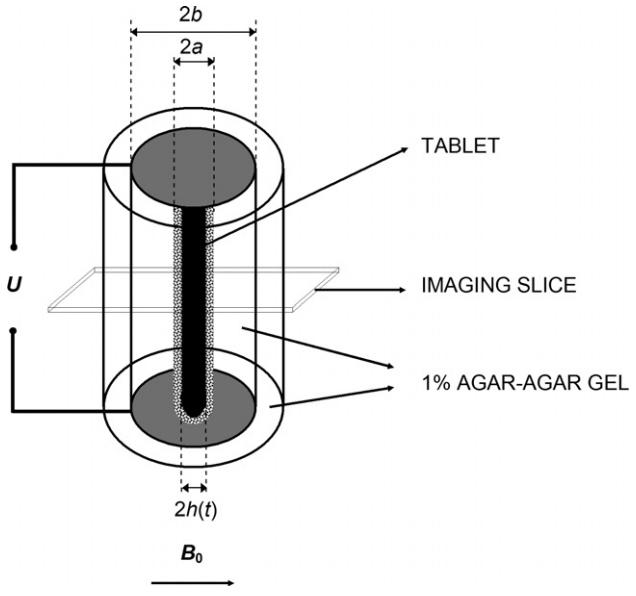

Fig. 1. The Plexiglas cell for tablet dissolution experiments. The cell has two concentric cylinders, each of length 12 mm. The inner cylinder of a diameter $2b = 10$ mm was capped at the ends with copper electrodes. The electrodes were connected to a voltage amplifier of a maximum output voltage of 220 V. The direction of the electric current was perpendicular to the static magnetic field B_0. The outer cylinder of 16 mm diameter was used as a reference with no electric current flowing through it. Both cylinders were filled with 1% agar–agar gel. A tablet with initial dimensions of diameter $2a = 4$ and 12 mm height was placed at the beginning of each experiment in the centre of the inner cylinder. During the experiment the tablet dissolved and at time t had a diameter $2h(t)$.

At low ion concentrations, the dependence of the diffusion coefficient on the ion concentration is weak and in the range of experimental error [26,27]. At very high ion concentrations the diffusion coefficient can become critically dependent on ion concentration. In our experiments the region of high ion concentration occurs only in the narrow layer close to the solid tablet. To simplify the model, the diffusion coefficient was assumed to be independent of ion concentration in the whole region. In this approximation the diffusion equation for cylindrical geometry is given by

$$\frac{\partial c_1(r,t)}{\partial t} = \frac{D}{r}\left[r\frac{\partial^2 c_1(r,t)}{\partial r^2} + \frac{\partial c_1(r,t)}{\partial r}\right] \quad \text{for } h(t) < r < b, \tag{1}$$

$$c_1(h(t),t) = C_N, \tag{2a}$$

$$\left.\frac{\partial c_1(r,t)}{\partial r}\right|_{r=b} = 0, \tag{2b}$$

$$c_1(r,0) = \begin{cases} C_0, & r \leqslant a, \\ 0, & a > r > b. \end{cases} \tag{3}$$

Here, c_1 denotes ion concentration, D the ion diffusion constant, C_0 the ion concentration in the solid tablet, a initial tablet radius, b inner cylinder radius, t_0 time in which the tablet is completely dissolved, and $h(t)$ the position of the tablet/gel boundary at time t. Mass conservation at the moving boundary $h(t)$ leads to the following equation [28] for the moving boundary position:

$$C_N\frac{\partial h(t)}{\partial t} = D\left.\frac{\partial c_1(r,t)}{\partial r}\right|_{r=h(t)}, \tag{4}$$

where C_N is the concentration of released ions that can freely diffuse per unit volume.

The diffusion equation (1) with the boundary conditions (Eqs. (2a) and (2b)) and the initial condition (Eq. (3)) was solved numerically with the finite difference method [28–30]. The cylinder radius r is divided into i space intervals Δr, and time is divided into j time intervals Δt. The concentration at a certain grid point $c_1(i\Delta r,(j+1)\Delta t)$ for a new time step can be calculated from Eq. (1) when the concentrations at the same grid point at the previous time step $c_1(i\Delta r, j\Delta t)$ and the concentrations of the nearest neighbours $c_1((i-1)\Delta r, j\Delta t)$ and $c_1((i+1)\Delta r, j\Delta t)$ are known. At time $t = 0$, the concentration profile is given by the initial condition (Eq. (3)). At boundaries $r = h(t)$ and $r = b$, the concentrations are given by Eqs. (2a) and (2b). After the concentration is calculated for each time interval, a new position of the moving boundary $h(t)$ is calculated using Eq. (4) and the grid is redistributed so that the boundary $h(t)$ is a nodal point. With a new grid the whole procedure for computing the concentration profile at a new time step is repeated until $h(t) \geqslant 0$ and the whole tablet dissolves.

After the whole tablet is dissolved no additional ions are released as the chemical reaction is complete and the only process involving ions is their diffusion between $x = 0$ and $x = b$. The concentration c_2 for times $t > t_0$ can then be calculated using Eq. (1) at boundary conditions

$$\left.\frac{\partial c_2(r,t)}{\partial r}\right|_{r=0} = \left.\frac{\partial c_2(r,t)}{\partial r}\right|_{r=b} = 0 \tag{5}$$

and the following "initial" condition at time $t = t_0$

$$c_2(r,t_0) = c_1(r,t_0). \tag{6}$$

The concentration profiles $c_2(r,t)$ for times larger than t_0 were also calculated numerically using the same numerical method as for $c_1(r,t)$.

3. Materials and methods

3.1. CDI

Electric currents flowing through a conductive sample induce a magnetic field in it. The induced magnetic field $\vec{B}_c$ is added to the static magnetic field $\vec{B}_0$ causing a shift ω_c in the Larmor frequency $\omega_c = \gamma B_c$; here γ is the gyromagnetic ratio of the nucleus. The induced magnetic field $\vec{B}_c$ is much smaller than the static magnetic field $\vec{B}_0$. The total magnetic field $\vec{B}_T = \vec{B}_0 + \vec{B}_c$ is therefore practically parallel to $\vec{B}_0$, and only the $\vec{B}_c$ component that is parallel to $\vec{B}_0$ contributes to the frequency shift ω_c. The frequency shift is obtained by measuring the phase shift $\varphi_c = \omega_c T_c$, where T_c is the total duration of the applied electric current pulses. Once the induced magnetic field B_c is known, the electric current density can be calculated using Ampere's law $\vec{j} = 1/\mu_0(\nabla \times \vec{B}_c)$. To obtain the image of a current density component j_z in the xy plane, two maps of the induced magnetic field ($\partial B_c^x/\partial y$ and $\partial B_c^y/\partial x$) are needed. Normally, this would imply sample rotation by 90° around the z axis. However, due to the cylindrical symmetry of the samples used in our experiments, only one image was needed to calculate the electric current density j_z. From the complex MRI signal $S = S_{\mathrm{Re}} + S_{\mathrm{Im}}$, an intermediate phase $\varphi_c' = \mathrm{arctg}(S_{\mathrm{Im}}/S_{\mathrm{Re}})$ with a range $0 \leqslant \varphi_c' < 2\pi$ was calculated first and then a phase image φ_c (with a continuous phase) was calculated from φ_c' by applying an unwrapping algorithm [31].

The applied DC-CDI pulse sequence is shown in Fig. 2. Electric current was applied to the sample by two external electrodes connected to a voltage supply generating electric pulses synchronously to the DC-CDI imaging sequence. The DC-CDI sequence is based on the conventional spin-echo imaging sequence to which two electric current pulses are added: one before and the other after the refocusing 180° RF pulse [1,2]. Both electric pulses have the same duration and amplitude, but opposite polarity to enable co-addition of phase shifts accumulated at each electric current pulse.

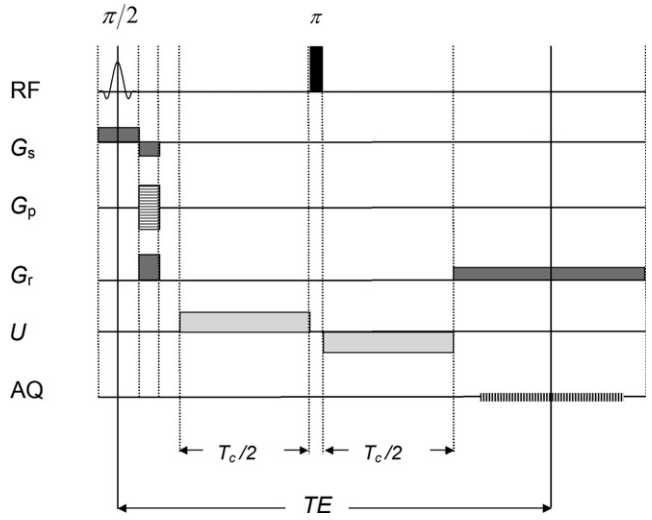

Fig. 2. The current density imaging (CDI) pulse sequence is based on the standard spin-echo pulse sequence to which two electric pulses of opposite polarity are added symmetrically to the π pulse. Each electric pulse has a duration of $T_c/2$.

3.2. Experiment

CDI experiments were performed on a 100 MHz Bruker Biospec system equipped with micro-imaging accessories. The experiments were carried out using a Plexiglas cell filled with 1% agar–agar gel. The cell contained two concentric cylinders. For CDI experiments, the inner cylinder of 10 mm diameter and 12 mm length was capped at the ends with electrodes, so that the electric current flowed along the axis of the cylinder. The electrodes were connected to an amplifier with a maximum output of 220 V. The outer cylinder (16 mm in diameter) was used as a reference, and was also filled with 1% agar–agar gel, but there was no current flow because there were no ions in this part of the sample (Fig. 1). A cylindrical tablet with diameter $2a = 4$ mm and of height $l = 12$ mm, was placed in the centre of the inner cylinder. Immediately after that, tablet dissolution started together with associated ion migration to the 1% agar–agar gel.

DC-CDI technique was employed to follow dissolution of a tablet in the gel. The technique detects conductivity changes in a sample that are closely related to the ion concentration in the sample. Tablets were made of various carboxylic acids (citric, oxalic, maleic, tartaric) which ionized on dissolution in the surrounding aqueous gel ($\mathrm{RCOOH} \rightarrow \mathrm{RCOO^-(aq)} + \mathrm{H^+(aq)}$), while a tablet made of sodium chloride dissolved with the release of hydrated ions to solution ($\mathrm{Na^+Cl^-(s)} \rightarrow \mathrm{Na^+(aq)} + \mathrm{Cl^-(aq)}$). The mobile ions formed by the dissolution of the tablet migrated into the gel surrounding the tablet and changed its conductivity. The dynamics of this process was followed by dynamic CDI. CDI images were acquired at regular time intervals of approximately 4 min until the tablet was completely dissolved and the current density was uniform everywhere in the gel. The imaging parameters were the field of view

$(FOV) = 25$ mm, matrix size 256×256, slice thickness $= 3$ mm, interecho time $(TE) = 32$ ms, repetition time $(TR) = 600$ ms and duration of current pulses $(T_c) = 20$ ms. The scan time for the CDI image was approximately 2.5 min.

To verify the mathematical model, for each CD image an average signal intensity was calculated as a function of the radial distance from the centre of the tablet. The intensities of all pixels having the same distance from the centre of the tablet were summed and divided by their number. The radial dependence of the CDI intensity thus obtained is directly proportional to the radial ion concentration dependences $c_1(r, t)$ for $t < t_0$ and $c_2(r, t)$ for $t > t_0$.

4. Results and discussions

Immediately after the tablet was inserted into the 1% agar–agar gel, it started to dissolve and released mobile positive and negative ions that began to migrate away from the tablet into the gel. The increased concentration of mobile ions altered the conductivity of the gel which was reflected in the CD image intensity. The CDI intensity was proportional to the electric current density in the sample and because of the homogeneous electric field E in the sample (which was produced by the two parallel electrodes), was also proportional to the concentration of positive and negative ions in the sample: $j = \sigma E = \alpha c$. Here σ is the electrical conductivity and α is a proportionality constant which depends on the applied voltage, the distance between the electrodes and the ion mobility. The constant α was determined from the measured current density at the time when the whole tablet was dissolved and the current density was uniform inside the inner cylinder. When the whole tablet was dissolved and the ions released were evenly distributed inside the inner cylinder, the ion concentration was calculated from the known mass of the tablet and the gel volume. For NaCl, the current density was 768 A/m^2 and the ion concentration was equal to 2.5 mol/L. From these data, the value for α was found to be 0.3 Am/mol.

Current density images thus show the progression of tablet dissolution and ion migration by direct measurement of the ion concentration (Fig. 3, second column), while magnitude images provide information only on the tablet size during dissolution (Fig. 3, first column). The concentration of positive and negative ions in the CD images is represented by different image gray levels (black: no electric current, i.e. no ions; white: maximum electric current, i.e. maximum ion concentration).

As the CDI scan time of 2.5 min was relatively long, ions might displace noticeably during scanning. To simplify mathematical analysis of the model, each CDI image was considered as being acquired at a time equal to the difference between mid-acquisition and the experiment start time. Diffusion constants for dissolved ions in the 1% agar–agar gel were calculated by finding the best fit of model concentration profiles $c_1(r, t)$ and $c_2(r, t)$ to the CDI data. As can be seen in the concentration profile plots in Fig. 3 (third column), the proposed model fits well the experimental data obtained by CDI. Significant dependence of the diffusion coefficient on the ion concentration exists only in a very narrow layer around the solid tablet. Only in this region are deviations of the theoretical model from the experimental data expected. Elsewhere, the ion concentration is low enough for the diffusion coefficient to be practically independent of ion concentration and the model agrees well with the experiment. Diffusion constants calculated from our measurements (D_M) are also in a good agreement with the diffusion constants for carboxylic acids and for sodium chloride in water given in the literature (D_L) [26,32] (Table 1).

The average concentrations of ions released from the tablet were calculated by integrating the ion concentration profiles over the sample volume. This was done for all CDI images of each experiment so the average ion concentration time dependence was obtained for dissolution of each tablet. Fig. 4 shows integrated CDI intensities within the inner cylinder as a function of time for dissolution of different carboxylic acid tablets and for the NaCl tablet. In all cases the average ion concentration first increases fast and at later times, when the tablet is practically completely dissolved, approaches a plateau.

The average ion concentration $Q(t)$ is proportional to the concentration of ions released from the tablet at time t. $Q(t)$ on the other hand is proportional to the volume change of the tablet during dissolution and can thus be described by

$$Q(t) = k(a^2 - h(t)^2), \tag{7}$$

where k is a proportionality constant, a the initial radius of the tablet and $h(t)$ the tablet radius at time t. Fig. 4 depicts the agreement between the measured average ion concentrations for different tablets and the model given by Eq. (7). The tablet radius $h(t)$ was obtained from the best fit of the theoretical model (Eqs. (1) and (4)) to the experimental data of the radial dependence of CDI intensity (Fig. 3, third column).

Drug release from tablets has been studied by various experimental methods. Some of these also provide spatial information; such methods are a combination of FTIR imaging and a dissolution test [33], and conventional ^{1}H MR imaging methods [34,35]. A combination of FTIR imaging in the ATR mode and a conventional dissolution test provides quantitative information of changes in the solid tablet as well as in the liquid phase. But the sensitivity of this method is limited when spectral bands overlap or when a material has weak infrared absorption. Conventional ^{1}H MRI can help in determining drug release from a tablet based on the signal loss at the position of the undissolved part of the tablet [34], as well as from changes of relaxation times in the solution due to the released part of the tablet. The relaxation properties can be significantly

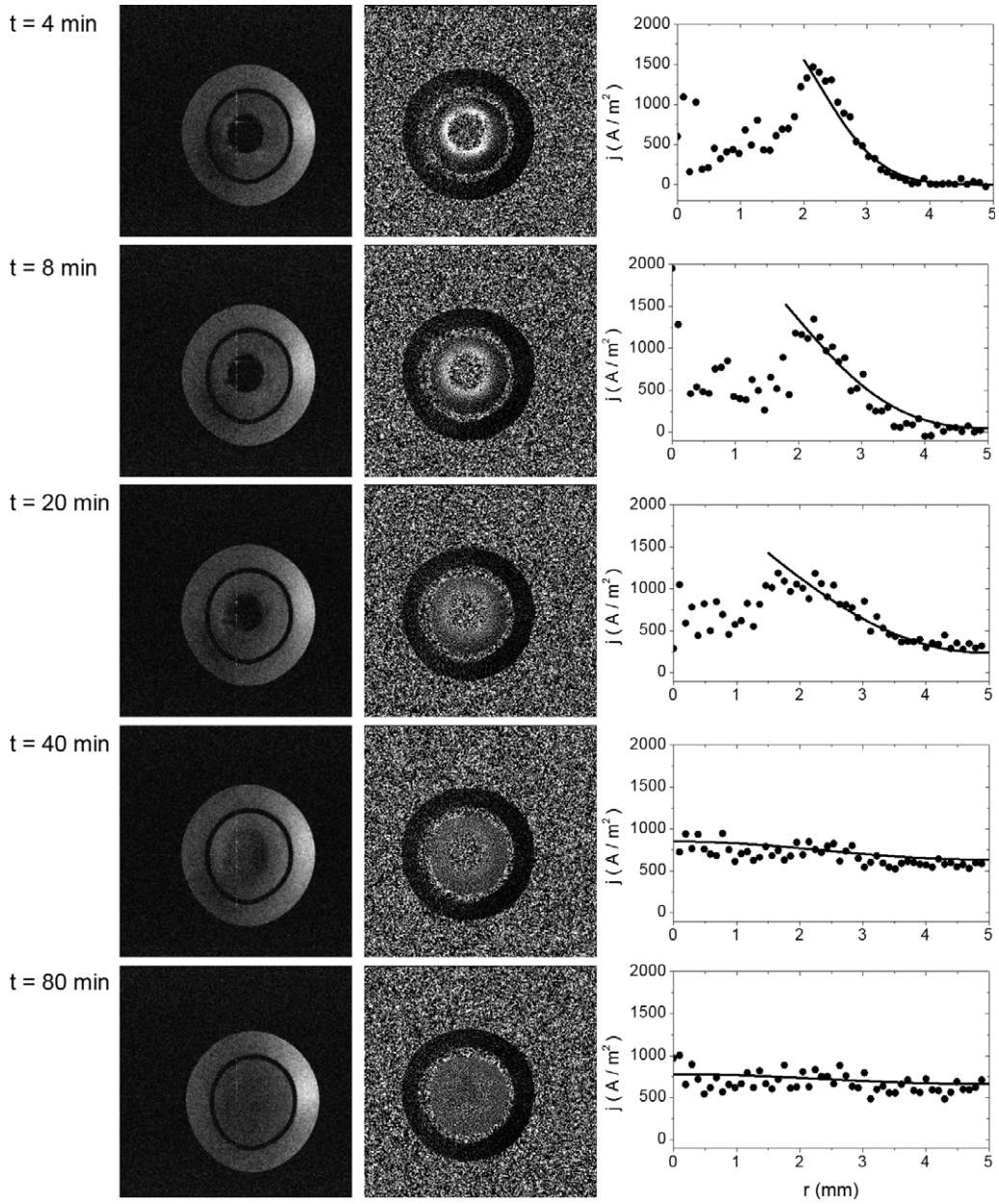

Fig. 3. Magnitude images (first column), current density images (second column), and current density as a function of radial distance from the tablet centre (third column, ● measured values, line: theoretical model) acquired at different times after the beginning of tablet dissolution. The sample consisted of a sodium chloride tablet dissolving in 1% agar–agar gel. The intensity of the CD images corresponds to the ion concentration (black: low ion concentration - no electric current, white: high ion concentration - maximum electric current). The imaging parameters were $FOV = 25$ mm, slice thickness = 3 mm, $TE = 32$ ms, $TR = 600$ ms, and $T_c = 20$ ms ($U = 220$ V).

Table 1
Measured diffusion constants (D_M) from CDI experiments and diffusion constants from literature (D_L) for tartaric, citric, oxalic, and maleic acids, and sodium chloride at room temperature

	D_M (10^{-9} m^2/s)	D_L (10^{-9} m^2/s)
NaCl	1.4 ± 0.2	1.5
Citric acid	0.8 ± 0.2	0.7
Maleic acid	0.8 ± 0.2	
Oxalic acid	1.5 ± 0.2	1.4
Tartaric acid	1.2 ± 0.2	0.8

changed if a gel is formed around the tablet. An example of this is a hydrophilic matrix tablet, where a gel of 5% polymer concentration has a value of T_2 reduced by threefold compared to the T_2 of water [35]. In our case, the relaxation effects are not so large. In the case of sodium chloride, the relaxation properties do not change with changing concentration of NaCl in the agar-agar gel. In the case of acids, changes in relaxation times were observed, but they are much smaller and do not enable small acid concentrations

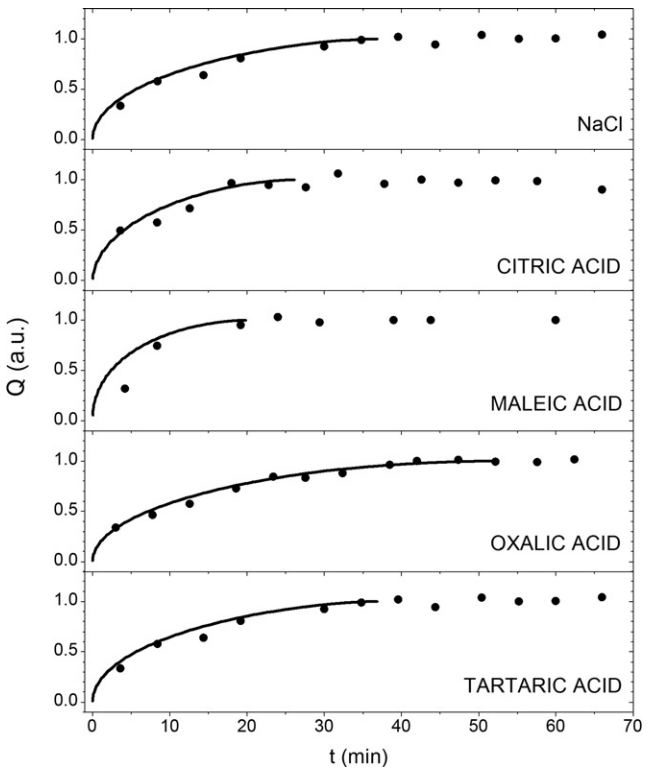

Fig. 4. Average ion concentration (integrated CDI intensity) as a function of time for sample tablets made of various acids (symbols: measured values, lines: theoretical values given by Eq. (7)).

to be determined in agar–agar gel. Measurements of relaxation changes based on ion concentration are less accurate than those obtained by CDI, where the ion concentration is measured directly. Selection of the most appropriate method for tablet dissolution studies very much depends on the problem. If a hydrogel is formed as in the case of hydrophilic matrix tablets, the relaxation properties are significantly changed, enabling tracing of gel formation by ^{1}H MRI. On the other hand, CDI is a more suitable method for cases when drug molecules dissolve to form ions and changes of relaxation properties are not sufficient to determine the presence of the drug in solution. Conventional MRI and CDI methods can be combined as well. For hydrophilic matrix tablets, for example, ^{1}H MRI could measure gel formation, while CDI could simultaneously measure the position of the released drug.

The major limitation in using the CDI method for *in vivo* biological studies is the inevitable need for a high voltage to produce large enough magnetic field changes induced by electric currents. In this study, an electric voltage of 220 V was used. The use of a high voltage was possible because it did not have any affect on the measured samples. The same results could also be obtained with a much lower voltage, but that would require signal averaging to improve the signal to noise ratio. For experiments on biological samples such a high voltage cannot be used as it would degrade the sample. Since biological samples are much more conductive at high frequencies than at low frequencies, a suitable technique for current density imaging of living systems is the RF-CDI technique [6,7,18] which operates in the radiofrequency range. The RF-CDI technique can still produce large enough electric currents at relatively low electric voltages. Another advantage of the RF-CDI technique is that it does not require sample rotation to perpendicular orientations to obtain CDI maps.

5. Conclusions

Dissolution and ion migration of tablets made of various acids and of sodium chloride were followed by CDI. This method enables monitoring of spatial and temporal changes of conductivity and is thus capable of detecting low concentrations of dissolved ions. In our experiment, CDI measurements were used to extract the diffusion constant of dissolved ions in a 1% agar–agar gel.

It was shown by a simple model of tablet dissolution that the CDI technique can be used for monitoring ion diffusion in the gel on the basis of conductivity changes. A potential use of the CDI technique is for monitoring the migration of ions through liquids and membranes. CDI is therefore a convenient technique for research in pharmaceutical sciences where drug release from tablets and the distribution of its molecules in tissues is important. These processes cannot be monitored efficiently by conventional MRI due to its low sensitivity to ion concentrations. CDI excels in this respect because it can also detect the ion distribution at low ion concentrations. CDI may therefore play an important role in monitoring free diffusion of electrically conductive substances through liquids, solids (tissue), and membranes, and can thus help in better understanding the transport of drug molecules in tissues.

References

[1] M.L. Joy, G.S. Scott, R.M. Henkelman, In vivo detection of applied electric currents by magnetic resonance imaging, Magn. Reson. Imag. 7 (1989) 89–94.
[2] G.C. Scott, M.L.G. Joy, R.L. Armstrong, R.M. Henkelman, Measurement of nonuniform current density by magnetic resonance, IEEE Trans. Med. Imag. 10 (1991) 362–374.
[3] G.C. Scott, M.L.G. Joy, R.L. Armstrong, R.M. Henkelman, Sensitivity of magnetic resonance current density imaging, J. Magn. Reson. 97 (1992) 235–254.
[4] I. Serša, O. Jarh, F. Demsar, Magnetic resonance microscopy of electric currents, J. Magn. Reson. 111A (1994) 93–99.
[5] U. Mikac, F. Demsar, K. Beravs, I. Serša, Magnetic Resonanance imaging of alternating electric currents, Magn. Reson. Imag. 19 (2001) 845–856.
[6] G.C. Scott, M.L.G. Joy, R.L. Armstrong, R.M. Henkelman, RF current density imaging in homogeneous media, Magn. Reson. Med. 28 (1992) 186–201.
[7] G.C. Scott, M.L.G. Joy, R.L. Armstrong, R.M. Henkelman, Rotating frame RF current density imaging, Magn. Reson. Med. 33 (1995) 355–369.
[8] D. Miklavčič, K. Beravs, D. Šemrov, M. Čemažar, F. Demsar, G. Serša, The importance of electric field distribution for effective in vivo electroporation, Biophys. J. 74 (1998) 2152–2158.
[9] K. Beravs, D. White, I. Serša, F. Demšar, Electric current density imaging of bone by MRI, J. Magn. Reson. Imag. 15 (1997) 909–915.

[10] K. Beravs, P. Oven, I. Serša, N. Torelli, F. Demsar, Electric current density imaging of oak (Quercus Rubra L.) Twigs by MRI, Holzforschung 52 (1998) 541–545.
[11] R.S. Yoon, T.P. DeMonte, K.F. Hasanov, D.B. Jorgenson, M.L.G. Joy, Measurement of Thoracic Current Flow in Pigs for the Study of Defibrillation and Cardioversion, IEEE Trans. Biomed. Eng. 50 (2003) 1167–1173.
[12] K. Beravs, A. Demšar, F. Demsar, Magnetic resonance current density imaging of chemical processes and reactions, J. Magn. Reson. 137 (1999) 253–257.
[13] U. Mikac, A. Demsar, I. Sersa, F. Demsar, Electric Current Density of tablet dissolution, Cell. Mol. Biol. Lett. 7 (2002) 136–138.
[14] I. Serša, K. Beravs, N.J.F. Dodd, S. Zhao, D. Miklavčič, F. Demšar, Electric current density imaging of mice tumors, Magn. Reson. Med. 37 (1997) 404–409.
[15] J.D.M. Thompson, M.L.G. Joy, R.M. Henkelman RM, Current density imaging in rabbit head and chest, in: Book of abstracts: Tenth Annual Scientific Meeting of the Society of Magnetic Resonance in Medicine, vol. 1. Berkeley, CA: SMRM; 1991, p. 1274.
[16] M.L.G. Joy, V.P. Lebedev, J.S. Gati, Imaging of current density and current pathways in rabbit brain during transcranial electrostimulation, IEEE Trans. Biomed. Eng. 46 (1999) 1139–1149.
[17] R.S. Yoon, M.L.G. Joy, Characterization of Spreading Depression in Rodent Neocortex, Using Radio Frequency Current Density Imaging, in: Proceedings of the International Society for Magnetic Resonance in Medicine, Seventh Scientific Meeting and Exhibition, Berkely, CA, ISMRM, 1999, p. 810.
[18] K. Beravs, R. Frangež, A.N. Gerkis, F. Demsar, Radiofrequency current density imaging of kainite-evoked depolarization, Magn. Reson. Med. 42 (1999) 136–140.
[19] E. Sallam, H. Ibrahim, R. Abu Dahab, M. Shubair, E. Khalil, Evaluation of fast disintegrants in terfenadine tablets containing a gas-evolving disintegrant, Drug. Dev. Ind. Pharm. 24 (1998) 501–507.
[20] N. Zao, L.L. Augsburger, Functionality comparison of 3 classes of superdisintegrants in promoting aspirin tablet disintegration and dissolution, AAPS Pharm. Sci. Tech. 6 (2005) E634–E640.
[21] Y. Bi, Y. Yonezawa, H. Sunada, Rapidly disintegrating tablets prepared by wet compression method: mechanism and optimization, J. Pharm. Sci. 88 (1999) 1004–1010.
[22] Y.X. Bi, H. Sunada, Y. Yonezawa, K. Danjo, Evaluation of rapidly disintegrating tablets prepared by a direct compression method, Drug. Dev. Ind. Pharm. 25 (1999) 571–581.
[23] K.S. Murthy, I. Ghebre-Sellassie, Current perspectives on the dissolution stability of solid oral dosage forms, J. Pharm. Sci. 82 (1993) 113–126.
[24] B.R. Rohrs, T.J. Thamann, P. Gao, D.J. Stelzer, M.S. Bergren, R.S. Chao, Tablet dissolution affected by a moisture mediated solid-state interaction between drug and disintegrant, Pharm. Res. 16 (1999) 1850–1856.
[25] S. Li, B. Wei, S. Fleres, A. Comfort, A. Royce, Correlation and prediction of moisture-mediated dissolution stability for benazepril hydrochloride tablets, Pharm. Res. 21 (2004) 617–624.
[26] J.R. Vinograd, J.W. McBain, Diffusion of electrolytes and of the ions in their mixture, J. Am. Chem. Soc. 63 (1941) 2008–2015.
[27] J.H. Wang, S. Miller, Tracer-diffusion in liquids. II. The self-diffusion as sodium ion in aqueous sodium chloride solutions, J. Am. Chem.Soc. 74 (1952) 1611–1612.
[28] J. Crank, The Mathematics of Diffusion, Claredon Press, Oxford, 1975.
[29] H.S. Carslaw, J.C. Jaeger, Conduction of Heat in Solids, Claredon Press, Oxford, 1959.
[30] F. Vermolen, K. Vuik, A numerical method to compute the dissolution of second phases in thermally alloys, J. Comp. Appl. Math. 93 (1998) 123–143.
[31] K. Itoh, Analysis of the phase unwrapping algorithm, Appl. Opt. 21 (1982) 2470.
[32] L. Börnstein, Physikalische Chemische Tabellen, Springer, Berlin, 1923.
[33] J. Van der Weerd, S.G. Kazarian, Combined approach of FTIR imaging and conventional dissolution tests applied to drug release, J. Controll. Rel. 98 (2004) 295–305.
[34] B.J. Fahie, A. Nangia, S.K. Chopra, C.A. Fyfe, H. Grondey, A. Blazek, Use of NMR imaging in the optimization of a compression-coated regulated release system, J. Controll. Rel. 51 (1998) 179–184.
[35] S. Baumgartner, G. Lahajnar, A. Sepe, J. Kristl, Quantitative evaluation of the polymer concentration profile during drug swelling of hydrophilic tablets using ^{1}H NMR and MRI methods, Eur. J. Pharm. Biopharm. 59 (2005) 299–306.